Valdez-Lopez, J. C., Donohue, M. W., Bok, M. J., Wolf, J., Cronin, T. W., & Porter, M. L. (2018). Sequence, Structure, and Expression of Opsins in the Monochromatic Stomatopod *Squilla empusa*. *Integrative and Comparative Biology*, *58*(3), 386-397. [icy007]. https://doi.org/10.1093/icb/icy007

Sequence, Structure, and Expression of Opsins in the Monochromatic Stomatopod *Squilla empusa*

Juan C. Valdez-Lopez[1†], Mary W. Donohue[1], Michael J. Bok[2], Julia Wolf[1], Thomas W. Cronin[1], Megan L. Porter[3]

[1]Department of Biological Sciences, University of Maryland Baltimore County

[2]School of Biological Sciences, University of Bristol

[3]Department of Biology, University of Hawai'i at Mānoa

[†]Corresponding author: 1000 Hilltop Circle Baltimore, MD 21250; juan5@umbc.edu; 240-455-3169;

Keywords: Squilla empusa, opsin, function, protein modeling

Abstract

Most stomatopod crustaceans have complex retinas in their compound eyes, with up to 16 spectral types of photoreceptors, but members of the superfamily Squilloidea have much simpler retinas, thought to contain a single photoreceptor spectral class. In the Atlantic stomatopod *Squilla empusa*, microspectrophotometry shows that all photoreceptors absorb light maximally at 517 nm, indicating that a single visual pigment is present in all photoreceptors in the retina. However, six distinct, but partial, long wavelength sensitive (LWS) opsin transcripts, which encode the protein component of the visual pigment, have been previously isolated through RT-PCR. In order to investigate the spectral and functional differences among *S. empusa's* opsins, we used RT-PCR to complete the 3' end of sequences for five of the six expressed opsins. The extended sequences spanned from the first transmembrane helix (TM1) to the 3' end of the coding region. Using homology-based modeling, we predicted the three-dimensional structure of the amino acid translation of the *S. empusa* opsins. Based on these analyses, *S. empusa* LWS opsins share a high sequence identity in transmembrane regions and in amino acids within 15Å of the chromophore-binding lysine on transmembrane helix 7 (TM7), suggesting that these opsins produce spectrally similar visual pigments in agreement with previous results. However, we propose that these spectrally similar opsins differ functionally, as there are non-conservative amino acid substitutions found in intracellular loop 2 (ICL2) and TM5/ICL3, which are critical regions for G-protein binding, and substitutions in extracellular regions suggest different chromophore attachment affinities. *In situ* hybridization of two of the opsins (Se5 and Se6) revealed strong co-expression in all photoreceptors in both midband and peripheral regions of the retina as well as in selected ocular and cerebral ganglion neuropils. These data suggest expression of multiple opsins - likely spectrally identical, but functionally different - in multiple types of neuronal cells in *S. empusa*. This suggests that the multiple opsins characteristic of other stomatopod species may have similar functional specialization.

Introduction

Stomatopod crustaceans, commonly referred to as mantis shrimps, make up a group of marine crustaceans that has been shown to have complex visual physiology, with up to 16 spectrally distinct photoreceptor classes observed in some species (Cronin et al. 1994; Cronin et al. 2010; Porter et al. 2009). Stomatopods have apposition compound eyes which are composed of many visual units called ommatidia (Marshall et al. 2007). Each ommatidium in the stomatopod eye has its own corneal and crystalline cone optical elements positioned above a rhabdom produced by seven or eight retinular photoreceptor cells (Marshall et al. 2007). In *Squilla empusa*, each rhabdom is formed by microvilli laden with visual pigments projected from seven photoreceptors, forming a single photoreceptive unit (Schönenberger, 1977). Visual pigments are composed of an opsin G-protein coupled receptor protein and a light sensitive chromophore. Upon photon absorption, the chromophore undergoes isomerization, typically from 11-*cis* retinal into all-*trans* retinal, and starts the phototransduction cascade. The spectral absorbance properties of visual pigments are typically tuned by alterations to the opsin residues that interact with and stabilize the chromophore in its binding pocket. Usually, one spectral class of photoreceptor expresses only one type of visual pigment (and thus a single opsin), although there is evidence for the expression of multiple distinct opsins within a single photoreceptor class from a number of species (e.g. African cichlid fish, Dalton et al. 2015; *Limulus polyphemus*, Battelle et al. 2016).

At the structural level, stomatopod compound eyes are characterized by having two peripheral regions (dorsal and ventral) bisected horizontally by an equatorial midband region of specialized ommatidia (Marshall et al. 2007). While the peripheral regions contain the typical crustacean set of two photoreceptors spectral types, one sensitive to violet or ultraviolet (UV) light and the second sensitive to blue-green wavelengths, photoreceptors within the midband row are typically specialized for polychromatic and polarization vision. Most stomatopod species (superfamilies Gonodactyloidea, Lysiosquilloidea, Pseudosquilloidea, and Hemisquilloidea) have six ommatidial rows in the midband region, but species in the Squillioidea, including *Squilla empusa* in the present study, have only two

ommatidial rows in the midband and are monochromatic (Schiff et al. 1986; Cronin, 1985). Phylogenetic studies of the stomatopods suggest that the common ancestor of the Squilloidea most likely had six midband rows (Ahyong, 1997; Porter et al. 2010). Thus, the two-row midband in Squilloidea is likely an evolved loss of photoreceptor diversity and spectral sensitivities. *S. empusa* are found near the coast of the Western Atlantic Ocean, from Maine to the Gulf of Mexico (Schiff et al. 1986). As is common in stomatopods, they make their homes by creating burrows on the ocean floor. Unlike stomatopods found in shallow coral reef habitats, *S. empusa* tends to burrow in muddy sea floors in dark and murky waters (Schiff et al. 1986). The limited light availability and their nocturnal hunting lifestyle (Schiff et al. 1986) may have contributed to the evolution of reduced visual complexity in *S. empusa*.

Microspectrophotometric (MSP) studies of *S. empusa* eyes showed that all retinal photoreceptors absorb light maximally at 517 nm (Cronin, 1985). The reduced complexity of the *S. empusa* retinal structure and the presence of a single spectral type of photoreceptor implies there is also a single expressed opsin in the retina that initiates a conserved visual phototransduction cascade. However, recent studies have suggested that *S. empusa* visual physiology could be more complex than previously thought. Porter et al. (2009) isolated six unique opsin sequences from *S. empusa* retinas that cluster with other crustacean long wavelength sensitive (LWS) opsins. This raises an interesting question—why would a species with a monochromatic visual system possesses multiple opsins? The first possibility could be that the opsins differ spectrally and when expressed together, they tune the photoreceptors to their maximal absorbance value. However, this typically leads to a broadened photoreceptor curve, and there is no evidence of multiple visual pigments with different absorbance peaks from past MSP studies (Cronin, 1985). Alternatively, the opsins could be identical, or highly similar, in spectral absorbance and yet differ functionally in how they initiate the phototransduction cascade due to structural differences leading to differences in membrane localization or chromophore coupling. There also exists the possibility that the opsins could be evolutionary vestiges, and are not translated into protein. In this study, we extended sequences of five opsin transcripts from Porter et al. 2009 to span from TM1 to the end of the coding

region in order to predict the opsins' functional and spectral differences. We also analyzed the expression of two of these opsins in *S. empusa* retinal and neural tissues. The data we present here suggest that *S. empusa* has multiple, spectrally-similar, but functionally distinct opsins expressed in the retina, optic lobes, and cerebral ganglion. We propose that this monochromatic stomatopod possesses a complex molecular toolkit of opsins, perhaps capable of complex visual system modulation and downstream processing.

Materials and Methods

RT-PCR (3'RACE) of S. empusa opsins mRNA and sequence analysis

S. empusa eyes were homogenized in TRIzol (Invitrogen) and RNA was extracted as per the TRIzol Reagent protocol (Invitrogen). Single strand cDNA was synthesized from isolated total RNA using the SuperScript RT III protocol (Invitrogen) and primers designed from published *S. empusa* opsin partial sequences (Porter et al. 2009; Table S1). After first strand synthesis, PCR was performed using Taq DNA polymerase (ThermoFisher Scientific) and specific primers for each of the six opsins identified in Porter et al. (2009) (Supplemental Table 1) to amplify opsin transcripts from the cDNA as per manufacturer's protocol (ThermoFisher Scientific). PCR amplicons were ligated into the pGEM-T Easy plasmid (Promega) via TA cloning using the manufacturer's protocol. Opsin sequences ligated into the plasmid were then sequenced (Genewiz). Partial opsin mRNA sequences obtained in Porter et al (2009) (GenBank accession numbers are the following: Se1-GQ221751.1, Se2-GQ221753.1, Se3-GQ221754.1, Se4-GQ221755.1, Se5-GQ221756.1, Se6-GQ221752.1) were aligned with sequences obtained through RT-PCR (3'RACE) using Geneious software, version R10 (Biomatters Limited) to complete the opsin's sequence. The mRNA sequences were then translated and aligned using Geneious software to facilitate the identification of non-conservative amino acid substitutions and other analyses.

Structural modelling and analysis of S. empusa opsins

122 The amino acid sequence for *S. empusa* opsin Se5 was used for homology-based three-
123 dimensional structural modeling using LOMETS software (Wu & Zhang, 2007). The *S. empusa* opsin
124 model was generated using squid (*Todarodes pacificus*) rhodopsin as a template (PDB ID 2ZIY)
125 (Shimamura et al. 2008). In combination with an amino acid alignment of the five analyzed opsins
126 (Figure 1), the model was used to identify amino acids proximal to the chromophore and potentially able
127 to alter visual pigment spectral tuning. While it is possible to spectrally tune an opsin without a non-
128 conservative amino acid substitution (Fasick & Robinson, 1998; Fasick & Robinson, 2000), charged
129 amino acids can alter spectral properties of the chromophore (Wang et al. 2014) and are identifiable
130 though bioinformatics. For our analysis, we considered non-conservative amino acid replacements, i.e.
131 i.e. positions in the amino acid alignment where the charged/non-charged property of the amino acid has
132 changed between opsins, within a 15Å (1.5 nm) distance capable of altering chromophore binding
133 chemistry. To generate the models of *S. empusa* opsin in complex with G-protein and arrestin, the *S.*
134 *empusa* opsin structural model was aligned with the crystal structure of human rhodopsin in complex with
135 mouse visual arrestin (PDB 4ZWJ) (Kang et al. 2015) and the crystal structure of human beta-2
136 adrenergic receptor in complex with bovine Gαs, rat Gβ, and bovine Gγ (PDB ID 3SN6) (Rasmussen et
137 al. 2011) using the cealign tool using Pymol software (Schrodinger). This was done to position *S. empusa*
138 opsin in complex with the signaling molecules. All amino acid numbering in this article is based on the *S.*
139 *empusa* opsin alignments (see Figure 1).
140
141 *Synthesis of riboprobes for in situ hybridization*
142 Riboprobes were synthesized for visual opsins Se1, Se5, and Se6, which represent representative opsins
143 from all three of the identified *S. empusa* opsin evolutionary clades identified in Porter et al. (2009). To
144 synthesize both sense and antisense probes, pGEM-T Easy plasmid DNA containing the 3'UTR of the
145 visual opsin transcripts were digested with one restriction enzyme (SalI or NotI) to create linear plasmids.
146 Next, the following in vitro transcription reaction was prepared: linear plasmid DNA, DIG-RNA

Labelling Mix (Roche), Polymerase buffer (Roche), RNase OUT (Invitrogen), and either T7 RNA polymerase or SP6 RNA polymerase (Roche). The transcription reaction was carried out as per the RNA polymerase protocol (Roche). Following transcription, reaction buffer with $MgCl_2$ (ThermoFisher Scientific) and 0.1 u/μL RNase-free DNase I, (ThermoFisher Scientific) was added to the mixture. The reaction was carried out as described in the RNase-free DNase I protocol (ThermoFisher Scientific). Riboprobes were purified using the RNeasy Minelute Cleanup Kit (QIAGEN).

Preparation of S. empusa tissue for in situ hybridization

S. empusa mantis shrimp were sedated on ice upon arrival. Specimens were decapitated by making a transverse cut to sever the nerve cord between the cerebral ganglion (CG) and subesophageal ganglion. Once the anterior portion of the cephalothorax was separated from the body, appendages were removed from the ophthalmic and antennular somites. The eyestalks (which include the optic lobes within) were cut away from the cephalothorax. The eyestalks and cephalothorax were fixed in 4% paraformaldehyde with 12% sucrose in 0.1% diethyl pyrocarbonate (DEPC) 1X phosphate-buffered saline (PBS) overnight at 4°C. For retinal only *in situ* hybridization studies, eyes were frozen and sectioned at 12-14 μm using a cryostat. Because of potentially lower signals expected from opsins expressed in neural tissues, isolated optic lobe and CG tissues were dehydrated using an ethanol gradient and propylene oxide, and then rehydrated, before being embedded in albumin gelatin. Then, the gelatin blocks were fixed overnight in 4% PFA in 0.1% DEPC 1X PBS, transferred to 0.1% DEPC 1X PBS, and sectioned at 60 μm using a vibratome.

In situ hybridization (ISH) of S. empusa tissue sections

Our protocol is based originally from Ishii et al. (2003), and was also used in Bok et al. (2014) and Cronin et al. (2010) for stomatopod retinas. For all probes, no probe and sense probe controls were run alongside antisense probes (Figures S3, S4). *S. empusa* sections on microscope slides were fixed in

4% PFA in PBS for 10 minutes. Next, the slides were washed three times in 0.1% (v/v) DEPC-1X PBS, 3 minutes per wash. The slides were then acetylated for 10 minutes in a solution containing 0.1% (v/v) DEPC-H_2O, triethanolamine, 0.02N HCl, and acetic anhydride, followed by three washes in 1X PBS, 5 minutes per wash. Hybridization solution (50% (v/v) formamide, 5X saline-sodium citrate (SSC) buffer, 5X Denhardt's solution, 250 μg/mL herring sperm DNA) was then added to the retina sections and the slides were incubated in a humidified chamber for 1 hour. Riboprobes were added to hybridization solution (150-200 ng riboprobe per 100 μL of hybridization solution for retinal tissue, and 100 ng riboprobe per 100 μL of hybridization solution for extraocular tissue) and were incubated at 70˚C for 10 minutes. The hybridization solution on the tissue was poured off and hybridization solution with riboprobe was added to the tissue sections. The slides were incubated at 75˚C overnight. The next day, slides were incubated in 0.2X SSC at 65˚C three times for 20 minutes to remove unbound probes. The slides were then incubated in Buffer B1 (0.1 M Tris pH 7.5 and 0.15M NaCl) for 5 minutes, and then in Buffer B2 (Buffer B1 and 10% normal goat serum) for 1 hour. Anti-digoxigenin-alkaline phosphatase (AP) (Roche) was diluted 1:5000 in Buffer B2 and was placed on the tissue sections, and the slides were incubated for 1-2 days at 4˚C. Slides were next washed with Buffer B1 4 times for three minutes each. Buffer B3 (0.1M Tris pH 9.5, 0.1M NaCl, 50 mM $MgCl_2$) was added to the slides and incubated for 5 minutes. Buffer B4 (NBT/BCIP tablet (Roche), 24 mg/mL levamisole) was then applied to the slides and left to incubate for several hours (retina sections) to overnight (extraocular tissue sections). Slides were then mounted and photographed via light microscopy.

Results

Amino acid sequence analysis of S. empusa opsins

Using RT-PCR of *S. empusa* eyes, we completed the 3' end of five of the six *S. empusa* opsin transcript sequences initially described by Porter et al (2009) (Figure 1). We were unable to amplify the 3' end of one of the six opsins (Se1), which is missing sequence data for part of TM6 and all of TM7, and

so was excluded from further analysis. Based on amino acid translations, these transcript sequences encode for seven-transmembrane (TM) opsins with a mean predicted molecular weight of 37.5 kDa. Also, the opsins contain the critical chromophore attachment site at K272 (numbering based on Figure 1 alignment), extended TM5 and TM6 helices (compared to bovine rhodopsin, Palczewski et al. 2000), a C-terminus region containing 9 or 10 putative sites of phosphorylation (Table 2), and important rhodopsin-class GPCR domains such as the (E)DRY motif on TM3 and NPXXY motif on TM7 (Figure 1).

Among the opsins analyzed there was high amino acid sequence similarity, with the sequence identity between opsins ranging from 76.6% to 93.7% (Figure S1). The percent identity across all opsins is 71.2%, with an average pairwise identity of 83.4%. Transmembrane domains also have a high degree of similarity, with percent identity of 76.3% and an average pairwise identity of 86.0%. Despite the high level of sequence identity we identified several sites of non-conservative amino acid substitution. Specifically, non-conservative substitutions exist at functionally relevant locations, including positions 74 on TM3; 112 on intracellular loop (ICL) 2; 189, 192, 199 on TM5; and 258 on TM7 (Table 1, Figure 1 and Figure 2A, 2B).

Structural modeling and analysis of a S. empusa opsin

A three-dimensional structural model was constructed for the amino acid sequence of opsin Se5, using homology to *Todarodes pacificus* rhodopsin, a rhabdomeric visual opsin, to predict the likely molecular conformation of opsins in *S. empusa*. The predicted structure of Se5 (Figure 2A, 2B)reveals a 7-transmembrane opsin with structured cytoplasmic protrusions. Specifically, the cytoplasmic protrusions of the extended TM5 and TM6 helices likely form a structural determinant for G-protein binding specificity, namely to Gαq (Porter et al. 2013, Donohue et al. 2017). The model also predicts a compact chromophore binding pocket (Figure 2C) comprised of all TM helices, and a chromophore binding site at K272 on TM7. The portions of the TM helices proximal to the extracellular space, and the ECLs

(particularly ECL2) form the opsin chromophore 'plug,' stabilized by a disulfide bond formed between C76 and C153.

To address the possibility that *S. empusa* opsins are spectrally distinct, we analyzed the identities of the amino acids proximal to the site of chromophore attachment on TM7, K272. Specifically, we considered non-conservative amino acid substitutions between opsins as possible sites of spectral tuning. For this analysis, we considered amino acids within a 15Å (1.5 nm) distance to be proximal, and potentially able to alter the chromophore binding chemistry. Our structural analysis suggests the opsins are spectrally identical or similar: no non-conservative amino acid substitutions were found in the within 15Å of K272 . Only one residue, site 74, has non-conservative amino acid substitutions within the 15Å distance of K272 (Figure 1, Figure 2A, Figure 2B). However, this site is unlikely to cause spectral shifts between opsins, given its position on TM3 where it's close to the extracellular space, and its R-group is almost completely out of the 15Å window (Figure 2A, Figure 2B). Interestingly, this site is placed close to the extracellular chromophore 'plug,' and while it isn't likely to affect the opsins spectrally, this site might serve as a tuning site for chromophore binding stability, a mechanism used in the mammalian rhabdomeric-type opsin, melanopsin (Tsukamoto et al. 2015). Additional analysis (Figure S5) reveals 11 amino acids surrounding the chromophore that are identical in all opsins analyzed in this study, and two are predicted to make contact with it (Y171 & W242). This analysis suggests a neutrally charged binding pocket similar to rhodopsin (Sakmar et al. 1989; Zhukovsky & Oprian. 1989), however, amino acids containing R-groups with hydroxl moieties are present in the pocket (Figure S5), such as Y171 (which is predicted to contact the chromophore), Y79, and Y245, which support a green shifted visual pigment (Chan et al. 1992; Asenjo et al. 1994).

We also considered whether or not the multiple opsins might differ functionally, even while sharing high sequence and structural similarity. Our structural and sequence analyses identified four sites of non-conservative amino acid substitutions: residues 112 on ICL2, residues 189 and 192 on TM5, and 199 on TM5/ICL3 (Figure 1, Figure 2A-F), located on important regions involved in coupling to

signaling molecules. Specifically, these regions (ICL2 & ICL3) recognize and bind the opsin's cognate G-protein, as shown extensively in bovine rhodopsin coupling to transducin (König et al. 1989; Franke et al. 1992; Yamashita et al. 2000; Natochin et al. 2003). We modeled the protein complex consisting of active-state *S. empusa* opsin and heterotrimeric G-protein (Gs was used in this model) (Figure 2D, Figure 2F). We observed the expected helical movement of TM5 and TM6 on the opsin and subsequent insertion of the C-terminus helix of Gα into the newly formed binding pocket in the opsin. Two of our sites, 112 on ICL2 and 199 on TM5 were particularly close to the binding pocket (Figure 2F). Residue 112 is of particular interest for two reasons: it is on an unstructured coil, which does not sterically hinder its R-group from potentially interacting with several residues on the G-protein.. Second, the non-conserved amino acid changes range from a complete switch of charge at that site (Se2 and Se6 are negatively charged, and Se3 is positively charged) to a loss of charge at that site (Se4 and Se5). Residue 199, while very close to the binding pocket, is hindered from movement due to its location on the cytoplasmic end of TM5. However, its proximity to the binding pocket might make it an important site that influences G-protein binding by impacting the overall charge of this region. Sites 189 and 192 are not likely to affect the G-protein binding pocket, but might affect the flexibility of TM5, and thus the formation of the binding pocket in the active state (Rasmussen et al. 2011).

We analyzed the C-terminus, specifically for the number of phosphorylation sites and how they might activate arrestin (Figures 2E and Figure 2G). All opsins had a similar number of possible phosphorylation sites and negatively charged residues, which work in a synergistic manner to activate arrestin (Zhou et al. 2017). More important than the total number of possible phosphorylation sites is their proximity to the positively-charged phosphorylation-sensing domain on arrestins (Table 2 and Figure 2G). To model opsin C-terminus-arrestin interaction and predict critical opsin C-terminus phosphorylation sites, we coupled active-state opsin to visual arrestin (crystal structure PDB 4ZWJ) (Figure 1, Figure 2E, G) and determined that opsin residues 308 to 322 were proximal to the positively-charged region on arrestin. These data suggest that possible phosphorylation sites within this region on

the opsin C-terminus are likely to be critical for signaling deactivation. Most opsins have a similar amount of possible phosphorylation sites in this region, except for Se3, which has most of its serines and threonines concentrated in this predicted critical region of arrestin interaction (Figure 1 and Table 2).

Expression of opsins in S. empusa retina and extraretinal neural tissue

Using the newly generated sequence data (Supplemental Figure 3), 3'UTR riboprobes were designed to hybridize to visual opsin mRNA in tissue sections *in situ*. Although riboprobes were synthesized for visual opsins Se1, Se5, and Se6, only Se5 and Se6 showed evidence of hybridization in our preparations. Expression patterns of *S. empusa* opsin transcripts Se5 (Figure 3A-D) and Se6 (Figure 3E-H) reveal that both opsins are robustly expressed in all regions of the retina–in both peripheral/hemispheric regions and in the midband. Expression of opsins Se5 and Se6 are also observed in transverse retinal sections (Figure 3B and Figure 3F), where riboprobe labeling is observed in all photoreceptors surrounding the rhabdoms in both hemispheres and in the midband (Figure 3C-D and Figure 3G-H). The intensity of Se5 labeling is even and robust in all regions of the retina (Figure 3C-D), and a similar expression pattern is observed for Se6 (Figure 3H). These data indicate that there is no preferential expression of either Se5 or Se6 in certain photoreceptors around the rhabdom in any region. Rather, *S. empusa* opsins Se5 and Se6 are co-expressed at high levels in all photoreceptors in all regions of the retina.

Given such robust co-expression of opsins in the retina, we then tested if the Se5 and Se6 opsins are expressed in extraretinal tissue, which is common in marine crustaceans (Donohue et al. 2017, Kingston & Cronin, 2016; Kingston et al. 2015) and terrestrial invertebrates such as *Papilio xuthus* (Arikawa et al. 2003). Through *in situ* hybridization of thicker (60 μm) tissue sections, we observed expression of retinal opsins Se5 and Se6 in other neural tissues (Figure 4). Specifically, expression of both opsin transcripts was observed in optic neuropils including the optic lobe lamina, medulla, and lobula, as well as the hemiellipsoid body in the lateral protocerebrum. Se6 was more broadly expressed

than Se5 in all neuropils, especially in the lamina and lobula neuropils (Figure 4). Neither Se5 nor Se6 opsin transcript expression were observed in the ventral eye, but it's possible that other opsins (not probed for in this study, such as Se2-Se4) are present. Se5 and Se6 opsin expression was also observed in the cerebral ganglion, specifically cell bodies that make up the olfactory neuropil (Figure 4). Thus, given all these results, co-expression of multiple opsins in this stomatopod is not only in photoreceptors, but surprisingly, also in downstream neurons involved in sensory processing.

Discussion

Past MSP analyses suggested that *S. empusa*, despite having two midband rows, has only a single photoreceptor spectral class (Cronin, 1985), in contrast to the large number of spectrally-distinct photoreceptor classes described in other stomatopod species (Cronin et al. 2010; Porter et al. 2009). These physiological data imply that a simple molecular composition exists in its photoreceptors (e.g. fewer expressed opsins), and in combination with past evolutionary studies (Porter et al. 2010) also suggest a reduction in eye complexity compared to stomatopods with many photoreceptor classes. Our data suggest quite the contrary, that the monochromatic *S. empusa* expresses multiple opsins in both retinal photoreceptor cells and downstream visual processing neurons (Figure 3, Figure 4). Homology modeling suggests that these opsins do not differ spectrally, but may differ functionally in phototransduction cascade interactions. The exact function(s) of these opsins in non-retinal tissue and the function of multiple opsins in a monochromatic retina remains unclear. It is also unknown whether or not the opsins expressed in non-retinal neurons bind chromophore and become functional visual pigments. Additionally, it's also unclear if these non-retinal neurons have the required signaling molecules to initiate canonical G-protein signaling. Transcripts putatively encoding the components of a Gq-mediated phototransduction pathway have been identified in other stomatopod species (Porter et al. 2013, Donohue et al. 2017). However, it is conceivable that opsins expressed in these non-retinal neuropils can initiate G-protein independent signal transduction, a well described and common mechanism (Heuss & Gerber, 2000;

Rajagopal et al. 2005; Shenoy et al. 2006). Thus, these findings of opsin expression in non-retinal neuropils, particularly in visual ones, might implicate these opsins in the inclusion of non-visual photoreception in visual pathways.

Co-expression of opsins in the retina, particularly spectrally similar ones, while an interesting finding, is a seemingly redundant mechanism of light detection in a monochromatic organism. However, our molecular modeling results also suggest that functional differences likely exist amongst the opsins, specifically, 'tuning' of chromophore, G-protein binding, and arrestin interactions via non-conservative differences in regions which form the respective binding pockets for each structure. Should the opsins differ functionally, as our analysis suggests, this could be an interesting mechanism to maintain stable visual function in different levels of irradiance. Specifically, our analysis suggests that non-conservative amino acid substitutions in extracellular residues of *S. empusa* opsins (74 and 258) might tune the stability of the 'chromophore plug' by affecting the binding affinity of the retinaldehyde chromophore (Tsukamoto et al. 2015; Janz & Farrens, 2004). This would alter the duration of the chromophore's attachment to the opsin, and thus make some opsins more sensitive to light than others (Tsukamoto et al. 2015). Thus, we propose that co-expression of spectrally identical opsins of varying sensitivity to light, or varying levels and times of activation, might be a mechanism *S. empusa* employs to maintain a stable visual representation of its environment at different times of day or in variable water depths.

For G-protein binding, comprehensive and comparative structural analysis (Flock et al. 2017) of GPCR-Gα binding suggest that residues in in ICL2, ICL3, and TM5 are at the interface between these two proteins. Our analysis has identified four residues of non-conservative amino acid substitution precisely at these structures in *S. empusa* opsins, residues 112 on ECL 2 and 189, 192, and 199 on TM5, which suggests they contribute either to G-protein docking and binding interactions, albeit through different mechanisms (Rasmussen et al. 2011). Therefore, we hypothesize that these sites serve as modulators of G-protein affinity and binding, causing differences in the electrical response of the photoreceptor, either in changes in strength or duration of light-induced depolarization. Additionally, the prolonged

depolarizing afterpotential - typical of invertebrate photoreceptors and induced when an extensive population of visual pigments is photo-converted into the active state (Johnson & Pak, 1986) - could be altered in opsins with a more transient or low affinity interaction with its cognate G-protein. Thus, opsin expressed in light-sensitive cells of the *S. empusa* retina and neuropils could have different capabilities to re-sensitize to high intensity light stimuli or have different onset kinetics of phototransduction.

Finally, based on the analysis of the number and position of serine and threonine residues in the C-terminus, deactivation or desensitization kinetics are likely to be similar amongst the opsins, with the exception of opsin Se3 where serines and threonines were concentrated in the predicted region of arrestin interaction. Therefore, we don't propose this as a common molecular mechanism of modulating phototransduction.

Summarizing our unexpected findings, we propose that the monochromatic Atlantic stomatopod *S. empusa* has a more complex visual system than predicted, based on its single retinal photoreceptor class. While we report co-expression of two opsins in the retina, the possibility of additional opsins should not be discounted. We also cannot discount the possibility of multiple opsins being evolutionary vestiges from ancestral stomatopods, where the complex eye conformation (ie. six midband rows between dorsal and ventral hemispheres) was likely the structure. This would represent a loss of molecular complexity in *S. empusa*, specifically in the array of opsins, that would mirror its structural eye loss. Thus, more work is required to ascertain if these multiple opsin transcripts are translated. Additionally, molecular analysis is needed to verify and substantiate our functional and spectral predictions. While stomatopod physiology proves difficult to study, electrophysiological studies of opsin expressing cells would shed light on the larger implications of opsin molecular adaptations. We propose that the expression of opsins in *S. empusa* is a flexible and versatile tool of not only mediating image formation in the retina, but of also adding nonvisual photoreceptive signals to downstream neurons. Given the unexpectedly large numbers of expressed opsins in many other species of stomatopods, including those

with far more complex retinas (Porter et al., 2009, 2013), we hypothesize that many mantis shrimps have functionally diversified opsins in their photoreceptor arrays.

Acknowledgements

We acknowledge NSF LSAMP BD Fellowship & NIH Training Grant T32 GM066706 awarded to JCVL, the awards generously made possible by Associate Vice Provost R. Garrison Tull and Professor K. Seley-Radtke, respectively. We also acknowledge UMBC's Applied Molecular Biology Program, where JCVL, JW, MJB, and TWC initiated this work. JCVL also acknowledges Professor Phyllis R. Robinson, for invaluable guidance, training, and support. This work was also funded by the Air Force Office of Scientific Research through Grant Number FA9550-12-0321.

382 **References**

383 Ahyong, S.T. 1997. Phylogenetic analysis of the stomatopoda (Malacostraca). Journal of Crustacean
384 Biology. 17: 695-715.

385 Arikawa, K., Mizuno, S., Kinoshita, M., Stavenga, D.G. (2003) Coexpression of two visual pigments in a
386 photoreceptor causes an abmormally broad spectral sensitivity in the eye of the butterfly *Papilio*
387 *xuthus*. The Journal of Neuroscience. 23: 4527-4532.

388 Asenjo, A.B., Rim, J., Oprian, D.D. (1994) Molecular determinants of human red/green color
389 discrimination. Neuron. 12: 1131-1138.

390 Battelle, B.A., Ryan, J.F., Kempler, K.E., Saraf, S.R., Marten, C.E., Warren, W.C., Minx, P.J., Montague,
391 M.J., Green, P.J., Schmidt, S.A., Fulton, L., Patel, N.H., Protas, M.E., Wilson, R.K., Porter, M.L.
392 2016. Opsin repertoire and Expression Patterns in Horseshoe Crabs: Evidence from the Genome of
393 *Limulus polyphemus* (Arthopoda: Chelicerata). Genome Biology and Evolution. 8: 1571-1589.

394 Bok, M.J., Porter, M.L., Place, A.R., Cronin, T.W. (2014) Biological sunscreens tune polychromatic
395 ultraviolet vision in mantis shrimp. Current Biology. 24: 1636-1642.

396 Chan, T., Lee, M., Sakmar, T.P. (1992) Introduction of Hydroxl-bearing Amino Acids Causes
397 Bathochromic Spectral Shifts in Rhodopsin. The Journal of Biological Chemistry. 267: 9478-9480.

398 Cronin, T.W. 1985. The visual pigment of a stomatopod crustacean, *Squilla empusa*. Journal of
399 Comparative Physiology A. 156: 679-687.

400 Cronin, T.W., Marshall, N.J., Land, M.F. 1994. The unique visual system of the mantis shrimp. American
401 Scientist. 82: 356-365.

402 Cronin, T.W., Porter, M.L., Bok, M.J., Wolf, J.B., Robinson, P.R. (2010) The molecular genetics and
403 evolution of colour and polarization vision in stomatopod crustaceans. Opthalmic and Physiological
404 Optics. 30: 460-469.

405 Dalton, B.E., Lu, J., Leips, J., Cronin, T.W., Carleton, K.L. (2015) Variable light environments induce
406 plastic spectral tuning by regional opsin coexpression in the African cichlid fish, Metriaclima zebra.
407 Molecular Ecology. 24: 4193-4204.
408 Donohue, M.W., Carleton, K.L, Cronin, T.W. (2017) Opsin expression in the central nervous system of
409 the s *Neogonodactylus oerstedii*. The Biological Bulletin. 233: 58-69.
410 Fasick, J.I. & Robinson, P.R. (1998) Mechanism of spectral tuning in the dolphin visual pigments.
411 Biochemistry. 37: 433-438.
412 Fasick, J.I. & Robinson, P.R. (2000) Spectral-tuning mechanisms of marine mammal rhodopsins and
413 correlations with foraging depth. Visual Neuroscience. 17: 781-788.
414 Flock, T., Hauser, A.S., Lund, N., Gloriam, D.E., Balaji, S., Babu, M.M. (2017) Selectivity determinants
415 of GPCR-G-protein binding. Nature. 545: 317-322.
416 Franke, R.R., Sakmar, T.P., Graham, R.M., Khorana, H.G. (1992) Structure and function in rhodopsin.
417 Studies of the interaction between the rhodopsin cytoplasmic domain and transducin. The Journal of
418 Biological Chemistry. 267: 14767-14774.
419 Heuss, C. & Gerber, U. (2000) G-protein-independent signaling by G-protein-coupled receptors. Trends
420 in Neurosciences. 23: 469-475.
421 Ishii, T., Hirota, J., and Mombaerts, P. (2003). Combinatorial coexpression of neural and immune
422 multigene families in mouse vomeronasal sensory neurons. Current Biology 13: 394– 400.
423 Janz, J.M. & Farrens, D.L. (2004) Role of the retinal hydrogen bond network in rhodopsin Schiff base
424 stability and hydrolysis. The Journal of Biological Chemistry. 279: 55886-55894.
425 Johnson, E.C. & Pak, W.L. (1986) Electrophysiological study of *Drosophila* rhodopsin mutants. Journal
426 of General Physiology. 5: 651-673.
427 Kang, Y., Zhou, X.E., Gao, X., He, Y., Liu, W., Ishchenko, A., Barty, A., White, T.A., Yefanov, O., Han,
428 G.W., Xu, Q., de Waal, P.W., Ke, J., Tan, M.H., Zhang, C., Moeller, A., West, G.M., Pascal, B.D.,
429 Van Eps, N., Caro, L.N., Vishnivetskiy, S.A., Lee, R.J., Suino-Powell, K.M., Gu, X., Pal, K., Ma, J.,

Zhi, X., Boutet, S., Williams, G.J., Messerschmidt, M., Gati, C., Zetsepin, N.A., Wang, D., James, D., Basu, S., Roy-Chaudhury, S., Conrad, C.E., Coe, J., Liu, H., Lisova, S., Kupitz, C., Grotjohann, I., Fromme, R., Jiang, Y., Tan, M., Yang, H., Li, J., Wang, M., Zheng, Z., Li, D., Howe, N., Zhao, Y., Standfuss, J., Diederichs, K., Dong, Y., Potter, C.S., Carragher, B., Caffrey, M., Jiang, H., Chapman, H.N., Spence, J.C., Fromme, P., Weierstall, U., Ernst, O.P., Katrich, V., Gurevich, V.V., Griffin, P.R., Hubbell, W.L., Stevens, R.C., Cherezov, V., Melcher, K., Xu, H.E. (2015) Crystal structure of rhodopsin bound to arrestin by femtosecond x-ray laser. Nature. 523: 561-567.

Kearse, M., Moir, R., Wilson, A., Stones-Havas, S., Cheung, M., Sturrock, S., Buxton, S., Cooper, A., Markowitz, S., Duran, C., Thierer, T., Ashton, B., Mentjies, P., & Drummond, A. (2012) Geneious Basic: an integrated and extendable desktop software platform for the organization and analysis of sequence data. Bioinformatics, 28: 1647-1649.

Kingston, A.C.N. & Cronin T.W. (2016) Diverse distributions of extraocular opsins in crustaceans, cephalopods, and fish. Integrative and Comparative Biology. 56: 820-833.

Kingston, A.C.N., Wardill, T.J., Hanlon, R.T., Cronin, T.W. (2015) An unexpected diversity of photoreceptor classes in the Squid, *Doryteuthis pealeii*. PLOS ONE. 10: e0135381.

König, B., Arendt, A., McDowell, J.H., Kahlert, M., Harvgrave, P.A., Hofmann, K.P. (1989) Three cytoplasmic loops of rhodopsin interact with transducin. PNAS. 86: 6878-6882.

Marshall, J., Cronin, T.W., Kleinlogel, S. (2007) Stomatopod eye structure and function: A review. Arthropod Structure & Development. 36: 420-448.

Natochin, M., Gasimov, K.G., Moussaif, M., Artemyev, N.O. (2003) Rhodopsin Determinants for Transducin Activation. The Journal of Biological Chemistry. 278: 37574-37581.

Palczewski, K., Kumasaka, T., Hori, T., Behnke, C.A., Motoshima, H., Fox, B.A., Le Trong, I., Teller, D.C., Okada, T., Stenkamp, R.E., Yamamoto, M., Miyano, M. (2000) Crystal structure of rhodopsin, A G protein-coupled receptor. Science. 289: 739-745.

454 Porter, M.L., Blasic, J.R., Bok, M.J., Cameron, E.G., Pringle, T., Cronin, T.W., Robinson, P.R. (2012)
455 Shedding new light on opsin evolution. Proceedings of the Royal Society B. 279: 3-14.
456 Porter, M.L., Bok, M.J., Robinson, P.R., Cronin, T.W. (2009) Molecular diversity of visual pigments in
457 Stomatopoda (Crustacea). Visual Neuroscience. 26: 255-265.
458 Porter, M.L., Speiser, D.I., Zaharoff, A.K., Caldwell, R.L., Cronin, T.W., Oakley, T.H. (2013) The
459 evolution of complexity in the visual systems of stomatopods: insights from transcriptomics.
460 Integrative and Comparative Biology. 53: 39-49.
461 Porter, M.L., Zhang, Y., Desai, S., Caldwell, R.L., Cronin, T.W. (2010) Evolution of anatomical and
462 physiological specialization in the compound eyes of stomatopod crustaceans. The Journal of
463 Experimental Biology. 213: 3473-3586.
464 Rajagopal, K., Lefkowitz, R.J., Rockman, H.A. (2005) When 7 transmembrane receptors are not G
465 protein-coupled receptors. The Journal of Clinical Investigation. 115: 2971-2974.
466 Rasmussen, S.G.F., DeVree, B.T., Zou, Y., Kruse, A.C., Chung, K.Y., Kobilka, T.S., Thian, F.S., Chae,
467 P.S., Pardon, E., Calinski, D., Mathiesen, J.M., Shah, S.T.A., Lyons, J.A., Caffrey, M., Gellman,
468 S.H., Steyaert, J., Skiniotis, G., Weis, W.I., Sunahara, R.K., Kobilka, B.K. (2011) Crystal structure of
469 the β2 adrenergic receptor-Gs complex. Nature. 477: 549-555.
470 Sakmar, T.P., Franke, R.R., Khorana, H.G. (1989) Glutamic acid-113 serves as the retinylidene Schiff
471 base counterion in bovine rhodopsin. PNAS. 86: 8309-8313.
472 Schiff, H., Abbott, B.C., Manning, R.B. (1986) Optics, range-finding, and neuroanatomy of a mantis
473 shrimp, *Squilla mantis* (Linnaeus) (Crustacea: Stomatopoda: Squillidae). Smithsonian Contributions
474 to Zoology. 440: 1-32.
475 Schönenberger, N. 1977. The fine structure of the compound eye of *Squilla mantis* (crustacea,
476 stomatopoda). Cell and Tissue Research 176: 205–233.

Shenoy, S.K., Drake, M.T., Nelson, C.D., Houtz, D.A., Xiao, K., Madabushi, S., Reiter, E., Premont, R.T., Lichtarge, O., Lefkowitz, R.J. (2006) β-Arrestin-dependent, G protein-independent ERK1/2 activation by the β2 adrenergic receptor. The Journal of Biological Chemistry. 281: 1261-1273.

Shimamura, T., Hiraki, K., Takahashi, N., Hori, T., Ago, H., Masuda, K., Takio, K., Ishiguro, M., Miyano, M. (2008) Crystal structure of squid rhodopsin with intracellularly extended cytoplasmic region. The Journal of Biological Chemistry. 283: 17753-17756.

Tsukamoto, H., Kubo, Y., Ferrens, D.L., Koyanagi, M., Terakita, A., Furutani, Y. (2015) Retinal attachment instability is diversified among mammalian melanopsins. The Journal of Biological Chemistry. 290: 27176-27187.

Wang, W., Geiger, J.H., Borhan, B. (2014) The photochemical determinants of color vision: Revealing how opsins tune their chromophore's absorption wavelength. Bioessays. 36: 65-74.

Wu, S. and Zhang, Y. (2007) LOMETS: A local meta-threading-server for protein structure prediction. Nucleic Acids Research. 35: 3375-3382.

Yamashita, T., Terakita, A., Shichida, Y. (2000) Distinct Roles of the Second and Third Cytoplasmic Loops of Bovine Rhodopsin in G Protein Activation. The Journal of Biological Chemistry. 275: 34272-34279.

Zhou, X.E., He, Y., de Waal, P.W., Gao, X., Kang, Y., Van Eps, N., Yin, Y., Pal, K., Goswami, D., White, T.A., Barty, A., Latorraca, N.R., Chapman, H.N., Hubbell, W.L., Dror, R.O., Stevens, R.C., Cherezov, V., Gurevich, V.V., Griffin, P.R., Ernst, O.P., Melcher, K., Xu, H.E. (2017) Identification of phosphorylation codes for arrestin recruitment by G-protein coupled receptors. Cell. 170: 457-469.

Zhukovsky, E.A. & Oprian, D.D. (1989) Effect of carboxylic acid side chains on the absorption maximum of visual pigments. Science. 246: 928-930.

TABLES

Table 1. Summary of non-conservative amino acid substitution amongst *S. empusa* opsins. Number, location, and identities of the amino acids are depicted, along with a hypothesized function of each amino acid of interest. Amino acids marked with (/) in a white cell indicate non-charged residues (includes polar and non-polar). Amino acids marked with (+) in a grey cell indicate positively-charged residues; and those marked with (-) in a black cell indicate negatively-charged residues. TM: Transmembrane region, ICL: Intracellular loop, ECL: Extracellular loop

Amino Acid of interest (Numbering based on alignment consensus)	Location on opsin	Se2	Se3	Se4	Se5	Se6	Hypothesized Function
74	TM3	Thr (/)	Arg (+)	Arg (+)	Thr (/)	Thr (/)	Chromophore binding stability
112	ICL2	Glu (-)	Lys (+)	Thr (/)	Thr (/)	Glu (-)	Modulation of Gα binding
189	TM5	His (+)	Phe (/)	Phe (/)	Tyr (/)	His (+)	Helical flexibilty
192	TM5	Ser (/)	Lys (+)	Lys (+)	Gln (/)	Ser (/)	Helical flexibilty
199	TM5	Lys (+)	Gln (/)	Lys (+)	Arg (+)	Lys (+)	Modulation of Gα binding
258	ECL3	Lys (+)	Lys (+)	Val (/)	Val (/)	Lys (+)	Chromophore binding stability

Table 2. Comparison and summary of C-terminus amino acids predicted to influence signaling deactivation in *S. empusa* opsins.

Squilla empusa opsin	Possible phosphorylation sites (Ser & Thr)	Possible phosphorylation sites in arrestin interacting region	Negatively charged amino acids (Asp & Glu)
Se2	9	5	8
Se3	10	8	6
Se4	10	5	8
Se5	10	5	8
Se6	9	6	7

FIGURE CAPTIONS

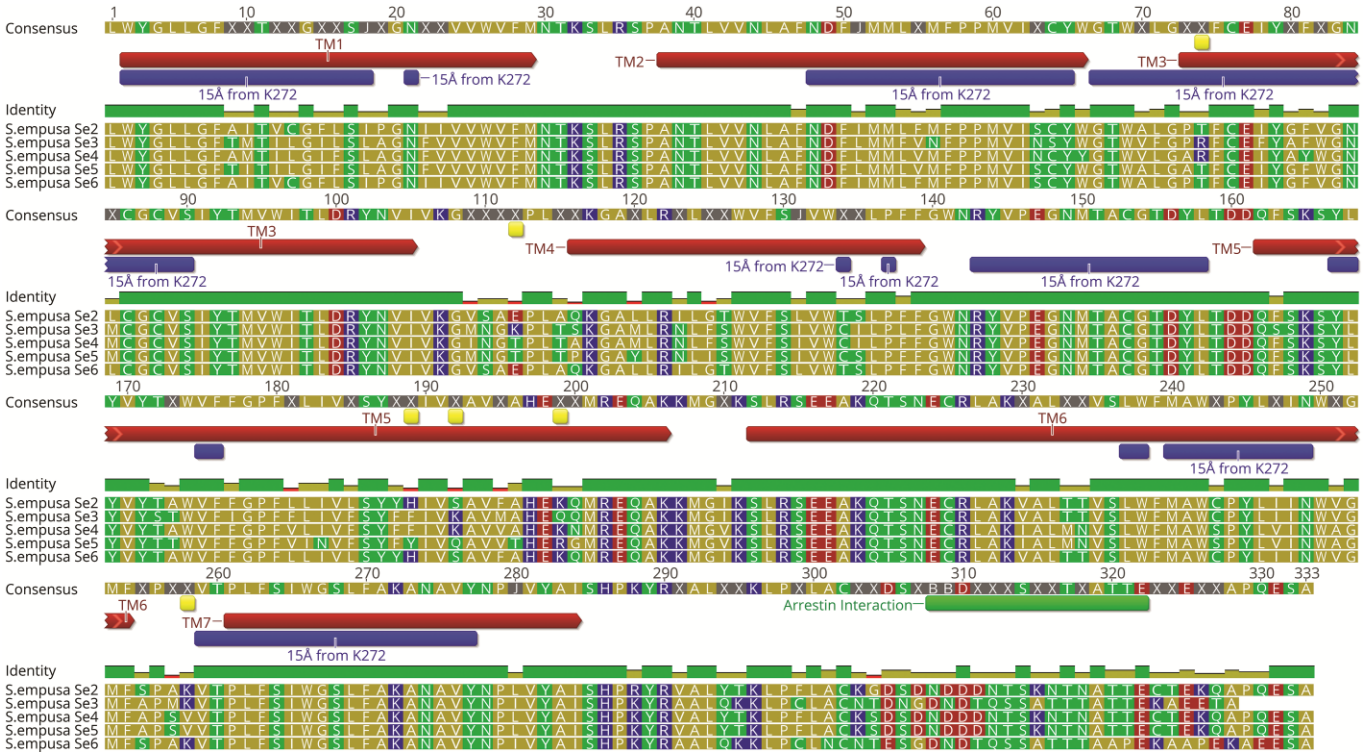

Figure 1. Amino acid sequence alignment of five *S. empusa* opsins. Opsin amino acid sequences were inferred from mRNA nucleotide sequences from Porter et al (2009) and RT-PCR performed in this study. Amino acid residues are colored according to their property—yellow: non-polar, green: polar and uncharged, and red and blue: charged (negatively and positively charged, respectively). High levels of sequence identity are observed throughout, particularly in the transmembrane regions (indicated by red annotations above the alignment) and in residues predicted to be in close proximity (≤15 Å) to the chromophore attachment site, K272 (indicated by blue annotations above the alignment). Sites of non-conservative amino acid substitutions amongst the opsins are denoted by the yellow annotations above the alignment. The green annotation above the alignment corresponds to residues predicted to be sites of phosphorylation and subsequent arrestin interaction.

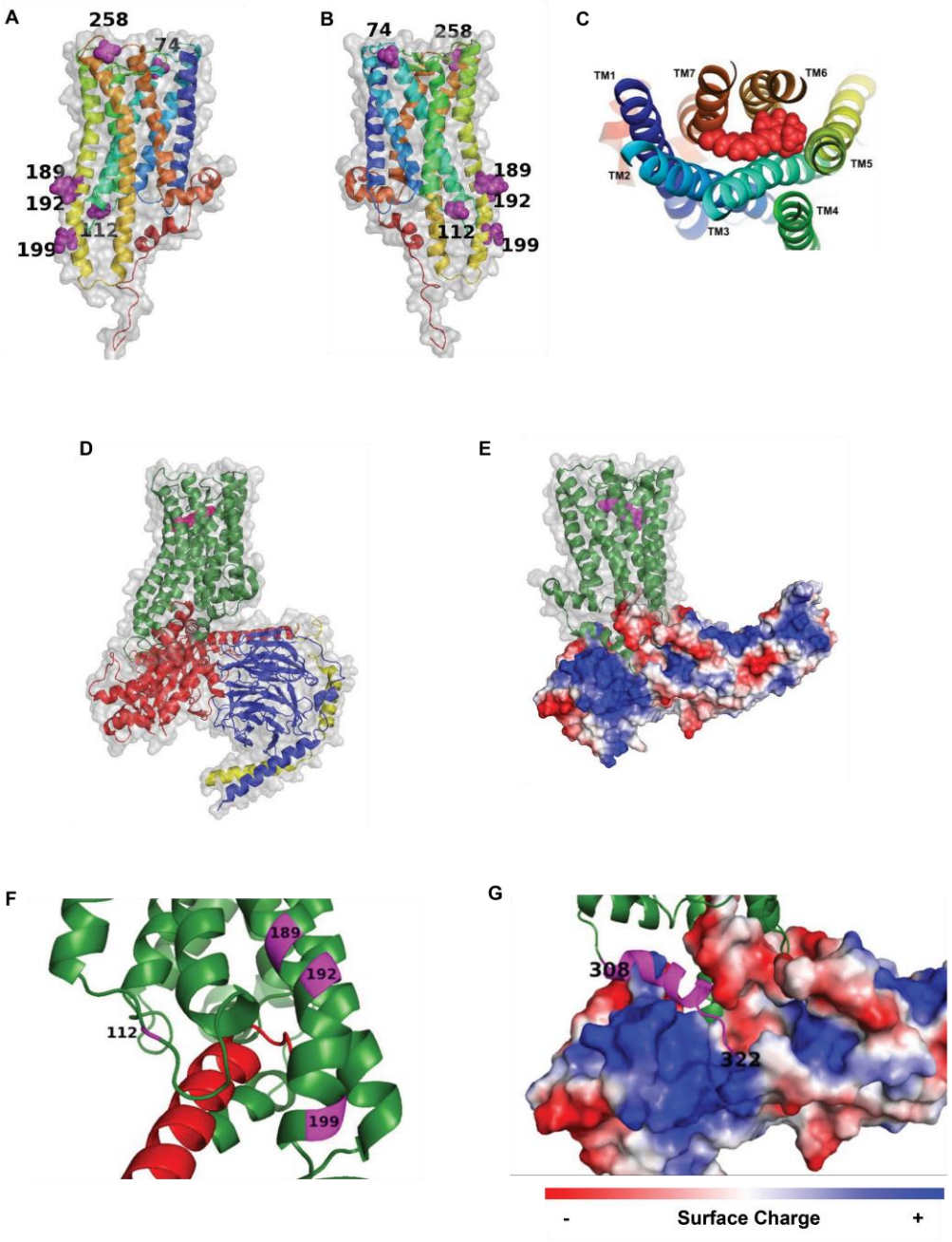

528

529 **Figure 2. Structural modeling of *S. empusa* opsins suggests amino acids sites of non-conservative**

530 **substitution function as modulators of G-protein binding and chromophore attachment stability.**

531 Front (A) and rear (B) view of structural model of *S. empusa* opsin Se5, labeling the predicted position of

the sites of non-conservative substitution on the opsin's tertiary structure (refer to Figure 1 for position of these sites on the opsin amino acid sequences). (C) Transmembrane helices form a compact binding pocket around the chromophore, 11-*cis* retinal (in red). No non-conservative amino acid substitutions are found within this binding pocket. (D) Model of active-state opsin bound to heterotrimeric G-protein (Gαs used in this model). (E) Model of active-state opsin in complex with arrestin (β-arrestin-1 used in this model). Surface charges plotted on arrestin—blue denotes positive charges and red denotes negative charges. (F) Four non-conservative amino acids substitutions are predicted to be proximal to the G-protein binding pocket, particularly amino acids 112 and 199, found on intracellular loops 2 and transmembrane helix 5, respectively. (G) The opsin's C-terminus is in close proximity to the positively-charged phosphate-sensing domains on arrestin. Acidic/negatively charged residues, serines, and threonines are concentrated in this region of the opsin's C-terminus.

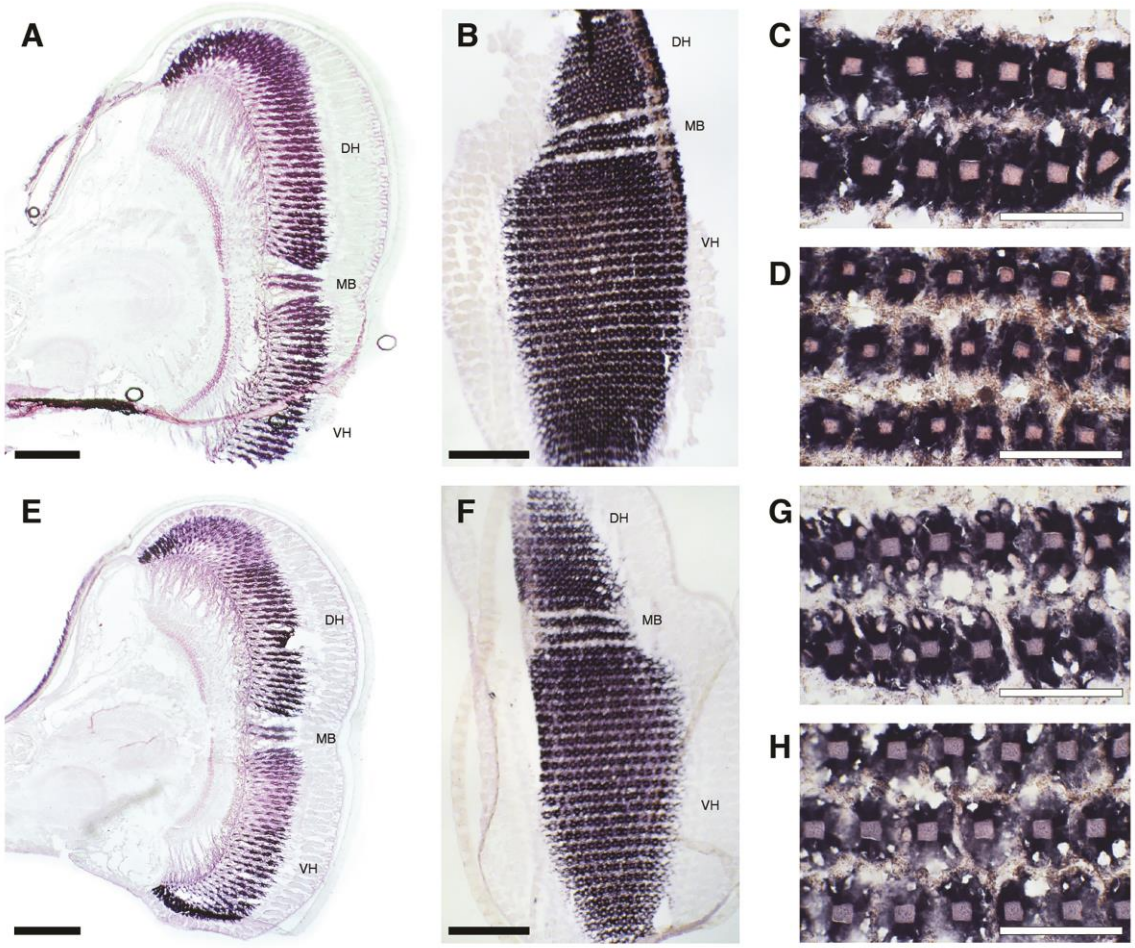

Figure 3. Robust transcript co-expression of M/LWS opsins Se5 and Se6 throughout the entire *S. empusa* retina. Sagittal (A & E) and transverse (B & F) retina sections labeled with Se5 (A-D) and Se6 (E-H) antisense riboprobes. Robust expression is observed in retina sections incubated with Se5 antisense riboprobes (A & B) including strong expression in all photoreceptors surrounding the rhabdom in the midband region (C) and periphery (D). Labeling with Se6 antisense riboprobes (E & F) also suggests robust expression of this opsin throughout the retina, with robust expression in all photoreceptors surrounding the retina in the midband region (G), and to a lesser degree in the periphery (H). DH: Dorsal hemisphere; MB: Midband; VH: Ventral hemisphere. Scale bars: A, B, E, F: 500 μm; C, D, G, H: 100 μm.

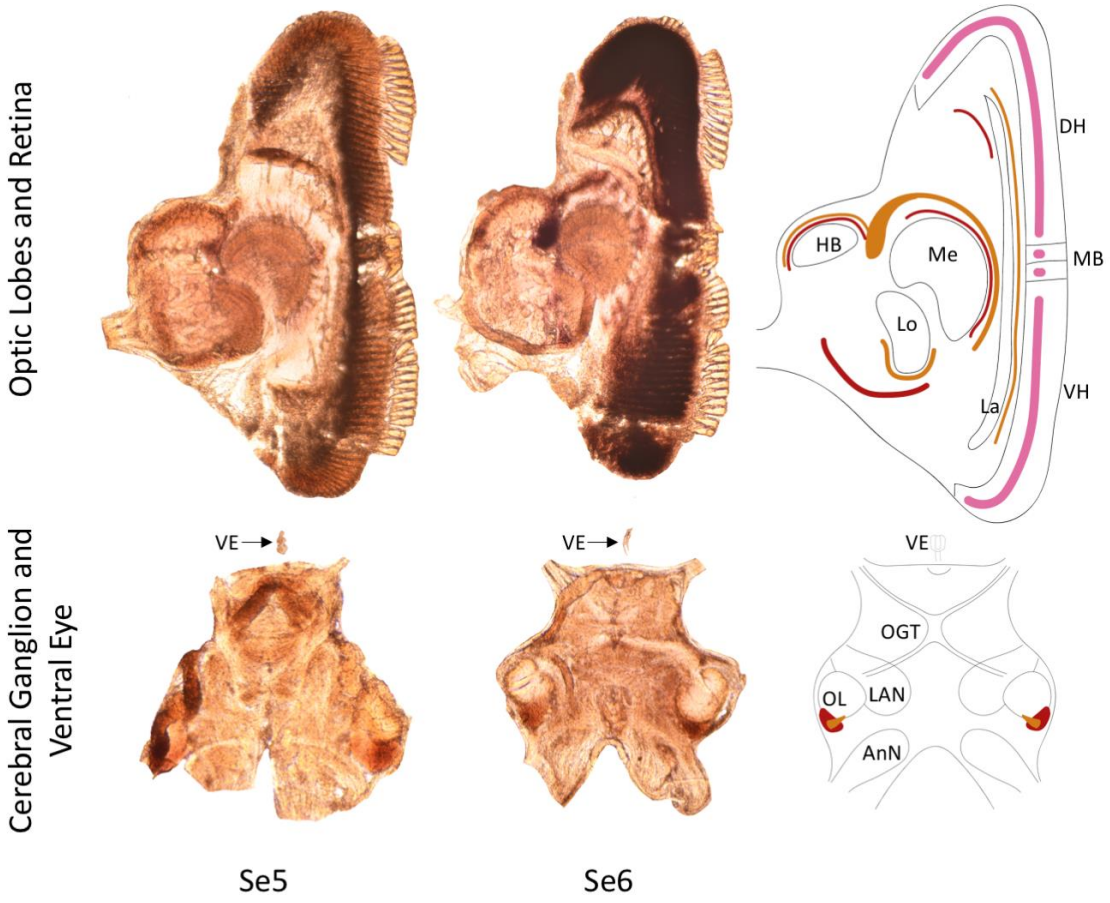

555

556 **Figure 4. Se5 and Se6 opsin transcripts are co-expressed the optic lobes and cerebral ganglion (CG)**
557 **of *S. empusa*.** Sagittal eyestalk sections (top row) suggest that Se5 and Se6 transcripts appear to trace the
558 lamina (La), medulla (Me), lobula (Lo), and hemiellipsoid body (HB) neuropils. As in Figure 3, both
559 transcripts are also co-expressed in retinal photoreceptors throughout the retina. Additionally, Transverse
560 CG sections show that Se5 and Se6 are co-expressed in the periphery of the olfactory lobes (OL).
561 Antennal neuropil, AnN; lateral antennal neuropil (LAN); olfactory-glomeruli tract (OGT); dorsal
562 hemisphere (DH); two equatorial midband rows (MB); and ventral hemisphere (VH).

563

564

565